Composite Structures 98 (2013) 153–159

Contents lists available at SciVerse ScienceDirect

Composite Structures

journal homepage: www.elsevier.com/locate/compstruct

Stretch–bend-hybrid hierarchical composite pyramidal lattice cores

Sha Yin [a,*], Linzhi Wu [a,*], Steven Nutt [b]

[a] Center for Composite Materials, Harbin Institute of Technology, Harbin 150001, China
[b] Department of Chemical Engineering and Materials Science, University of Southern California, Los Angeles, CA 90089-0241, USA

ARTICLE INFO

Article history:
Available online 23 November 2012

Keywords:
Carbon fibers
Composite lattice
Hierarchy
Optimization
Structural efficiency

ABSTRACT

Hierarchical composite pyramidal lattice (CPL) cores with foam-core sandwich struts were designed, and two stacking patterns were fabricated and tested in out-of-plane compression. Analytical expressions for five possible failure modes were derived considering not only stretching and bending deformation but also shear deformation of struts. Core shear failure was absent from collapse mechanism maps for both Patterns-I and II CPL cores. Optimized Pattern-I hierarchical CPL cores were more efficient than Pattern-II cores. The following comparison with almost all competing composite sandwich cores revealed that the hierarchical CPL structures here, the assembly of both stretch- and bend-dominated constructions, could perform among the most efficient sandwich cores. Meanwhile, the construction concept can also enable multifunctionality by judicious selection of strut core materials without compromising structural efficiency.

© 2012 Elsevier Ltd. All rights reserved.

1. Introduction

Stretch-dominated lattices are well-suited to lightweight structural designs because of their high efficiency and multifunctional potential [1]. Composite lattices are hybrids of fibrous composites and optimized lattice topologies, and thus more efficient than their homogeneous counterparts because of the high specific properties of the parent materials. In the last decade, fabrication techniques, and mechanical properties for such lattices have been reported [2–8]. These structures have filled gaps in the material property space, enlarging the material selection range for designers and demonstrating the potential for deployment in future applications. However, the high-efficiency structures with ultra-low densities ($\bar{\rho} < 5\%$) are prone to buckling. Several strategies have been pursued to improve the mechanical behavior of these structures. In one example, by sectional designing, hollow composite pyramidal lattice (CPL) cores were designed and produced using a thermal expansion molding technique [9]. In that work, the out-of-plane compressive strength of hollow CPL cores was reportedly about twice that of solid truss counterparts [6], and the specific strength surpassed that of the world's lightest structures [10].

Structural hierarchy is a common strategy employed with great success in natural materials (e.g., wood and bone) and in some engineering structures, resulting in exceptional efficiency and increased buckling strength. Hierarchical structures can be achieved by assembling stretch- or bend-dominated cellular materials and sandwich structures thereof at different length scales, including a self-similar hierarchical corrugated sandwich core [11], a corrugated sandwich core with foam sandwich struts [12,13], and a hierarchical honeycomb core [14]. In one report, a self-similar corrugated core was 10 times stronger than a traditional corrugated core of the same relative density [11]. Since the stretch-dominated materials (such as lattice structures) are generally more efficient than their bend-dominated counterparts (such as foams), it is readily to expect that the stretch–stretch-hybrid hierarchical structures (in a recent work [15]) should be more efficient than other assemblies. However, such structures based on the present technology [9] are of greater length scale for conventional application. It is generally difficult and costly to control the length scale of periodic lattice materials and the composing hierarchical structures, and almost impossible to produce such materials of the same pore scale as foams.

Accordingly, in the present work, we report efforts to produce a stretch–bend-hybrid hierarchical core by employing foams, the cell wall strut length scale of which is smaller than trusses of traditional lattice material. Then in this case, the macroscopic sandwich core is a pyramidal lattice which is stretch-dominated, while the mesoscopic sandwich core of the pyramidal strut is bending dominated foam of lower efficiency. Two configurations for the stretch–bend-hybrid hierarchical core are described along with two corresponding fabrication methods, and selected samples are tested in out-of-plane compression. Analytical predictions for compressive properties are presented, collapse mechanism maps are constructed, and structural efficiency after optimization is evaluated and compared with competing core topologies.

* Corresponding authors. Tel.: +86 451 86412549; fax: +86 451 86402739.
E-mail addresses: yinsha2008@gmail.com (S. Yin), wlz@hit.edu.cn (L. Wu).

0263-8223/$ - see front matter © 2012 Elsevier Ltd. All rights reserved.
http://dx.doi.org/10.1016/j.compstruct.2012.11.004

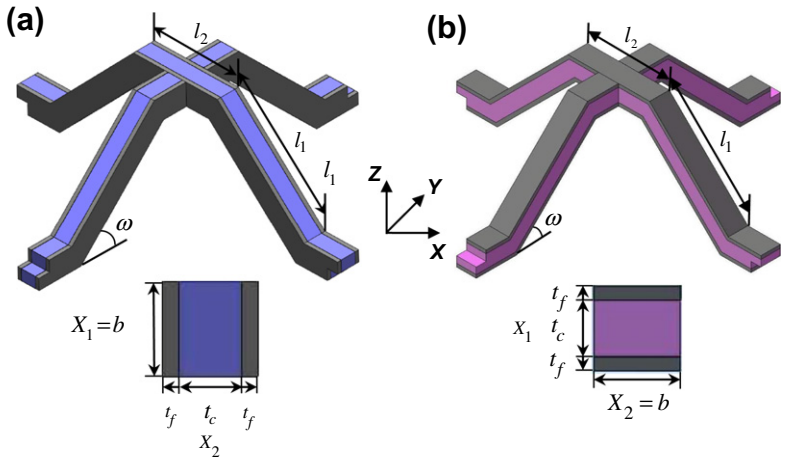

Fig. 1. Representative unit cells for two stacking patterns of hierarchical composite pyramidal cores together with the corresponding strut cross sections.

Table 1
Mechanical properties of carbon fabric prepreg.

Property	Value
Tensile strength (MPa)	756
Tensile modulus (GPa)	69
Compression strength (MPa)	557
Compression modulus (GPa)	64
In-plane shear strength (MPa)	118
In-plane shear modulus (GPa)	4.2
Interlayer shear strength (Mpa)	68
Poisson's ratio	0.064

2. Structural configurations and experimental approaches

Two kinds of foam sandwich configurations are developed to produce hierarchical CPL cores, and representative unit cells are shown schematically in Fig. 1, along with the corresponding sections of the foam-core sandwich struts. The stacking manners of foam sandwich strut are different for the two configurations: the stacking in Fig. 1a is in the *X*–*Y* plane (in-plane stacking), while in Fig. 1b is along *Z*-direction (out-of-plane stacking). These two constructions can be achieved by different fabrication approaches. One approach employs flat foam sandwich plates, and the other involves corrugated foam sandwich plates, as described in the following section. PMI foams (Rohacell 71WF-HT) were chosen for the low density ($\rho_c = 75$ kg/m^3) and the capacity to sustain a pressure up to 0.5 MPa at 125 °C. The face sheets of the foam sandwich were produced from plain-weave carbon fabric prepreg (3234/G803) of density $\rho_f = 1550$ kg/m^3, and the mechanical properties were presented in Table 1.

2.1. Approach I – flat foam sandwich plate

Flat foam sandwich plates were produced by hot-pressing and cutting into strips, as shown in Fig. 2a. The strips were joined together by slot insertion at the nodes to form the stretch–bend hierarchical pyramidal core shown in Fig. 2b (epoxy adhesive was applied at the slots to secure the nodes). The representative unit cell of this Pattern-I hierarchical composite pyramidal core is shown in Fig. 1a.

2.2. Approach II – corrugated foam sandwich plate

In this approach, we first fabricated a corrugated foam sandwich plate using a corrugated steel mold, as shown in Fig. 3a. Plies of fabric prepreg were stacked on the steel mold, followed by a foam strip cut from a foam block (using a hot wire). An equal number of prepreg plies were then laid on the foam strip. Next, strips of equal width were cut from the corrugated foam sandwich plate (Fig. 3b). Finally, these strips were fit together by slot insertion at the pyramidal nodes. The representative unit cell for the Pattern-II hierarchical CPL cores was shown in Fig. 1b.

2.3. Relative density

The relative density, $\bar{\rho}$, can be expressed as:

$$\bar{\rho} = \frac{2b\left[l_1 + l_2 - X_1 \tan\frac{\omega}{2}\right](2t_f\rho_f + t_c\rho_c)}{\left[l_1\cos\omega + l_2 - X_1\tan\frac{\omega}{2}\right]^2(l_1\sin\omega + X_1)} \quad (1)$$

where l_1 is the strut length, l_2 is the length of the horizontal trusses which connects the inclined struts at the pyramidal node and ω is the inclination angle between the struts and the base of the unit cell. The thickness and density of the foam core of the sandwich strut is t_c and ρ_c, while the face sheet thickness and density is t_f and ρ_f. For Pattern-I CPL cores, one side of the strut section is defined as $X_1 = b$, and the other as $X_2 = (2t_f + t_c)$; while for Pattern-II CPL cores, $X_1 = (2t_f + t_c)$ and $X_2 = b$.

2.4. Out-of-plane behavior

The stretch–bend-hybrid hierarchical CPL cores were bonded with two carbon fiber face sheets using adhesive film (J-272, Heilongjiang Institute of Petrochemical) to form sandwich structures. Through-thickness compression tests were performed at a displacement rate of 0.5 mm/min at room temperature using a screw-driven testing machine (INSTRON 5569) with load capacity of 50 kN following ASTM C365/C 364M-05 [16]. The measured compressive response is plotted in Fig. 4a along with the theoretical prediction. Note that the measured compressive modulus and strength of the face sheet of the foam sandwich is $E_f = 16.5$ GPa, $\sigma_f = 267$ MPa. The nominal stress increases almost linearly with the nominal strain and reaches a peak. For Pattern-I CPL cores, face sheet wrinkling of the sandwich strut occurred at the peak, manifest as a sharp drop in supported load, while shear buckling occurred for Pattern-II CPL cores. Failure of the CPL cores occurred at a strain $\varepsilon \approx 0.025$, as shown in Fig. 4b and c. The measured failure loads differ from predicted values by 22.2% for specimen A (Pattern I) and by 15.4% for specimen B (Pattern II). The difference here is acceptable. Surface damage from cutting of the foam sandwich strips during preparation could be one reason that account

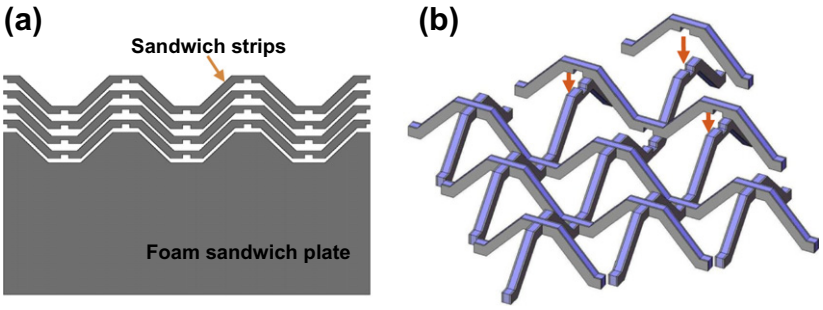

Fig. 2. Fabrication approach with flat foam sandwich plate (Pattern I): (a) cutting foam sandwich strips; and (b) strips slotting together.

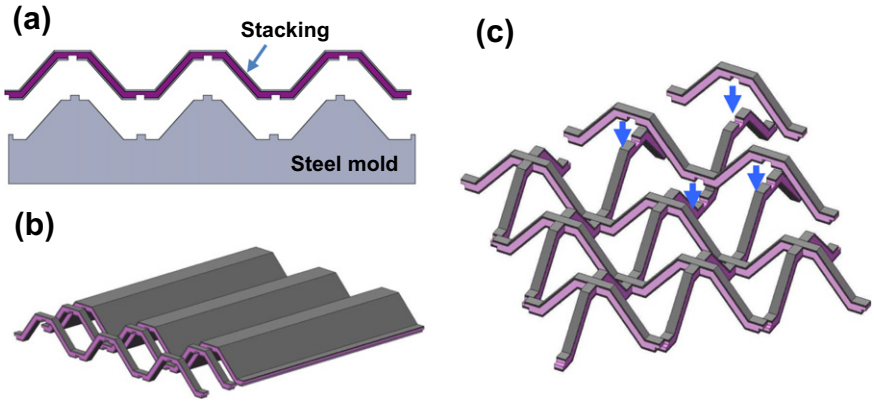

Fig. 3. Fabrication approach with corrugated foam sandwich plate (Pattern II): (a) fabricating a corrugated foam sandwich plate with a specially designed steel mold; (b) cutting foam sandwich strips; and (c) strips slotting together.

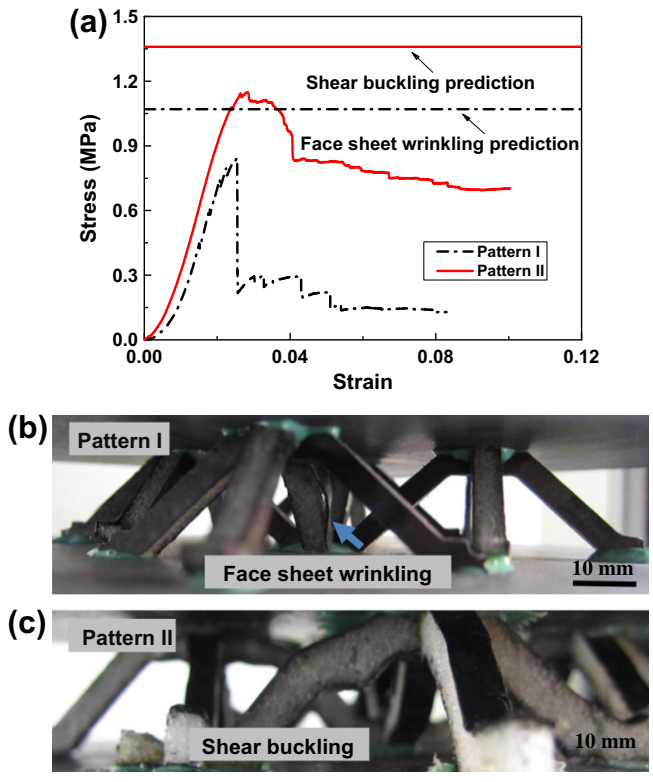

Fig. 4. (a) Measured compressive response of the hierarchical CPL cores with foam sandwich struts included with analytical predictions; and the corresponding dominant failure modes of: (b) Pattern-I CPL core and (c) Pattern-II CPL core.

for the lower property values observed, and thus should be pay more attention in the fabrication approach. Geometries of the selected representative structures along with the measured and predicted peak strengths are summarized in Table 2.

3. Analysis

3.1. Properties of foam

The selected foam (Rohacell WF-HT) is a closed-cell rigid foam based on PMI (polymethacrylimide) chemistry. For closed-cell foams, Gibson and Ashby have shown that the elastic properties strongly depend on the relative density $\bar{\rho}_c = \rho_c/\rho_s$, where ρ_s is the density of the parent polymer. Young's modulus E_c, shear modulus G_c and shear strength τ_c is given by:

$$\frac{E_c}{E_s} \approx \phi^2 \bar{\rho}_c^2 + (1-\phi)\bar{\rho}_c \tag{2}$$

$$G_c \approx \frac{3}{8} E_c \tag{3}$$

$$\frac{\tau_c}{\sigma_s} \approx 0.2\phi^{3/2}\bar{\rho}_c^{3/2} + (1-\phi)\bar{\rho}_c \tag{4}$$

where E_s and σ_s is Young's modulus and strength of the parent polymer, and ϕ is the volume fraction of cell wall material in a unit cell [17]. In the present study, we assume $E_s = 3600$ MPa, $\sigma_s = 60$ MPa, $\rho_s = 1250$ kg/m^3 and $\phi = 0.6$. For the selected foam (Rohacell 71WF-HT), the measured density $\rho_c = 75$ kg/m^3, $E_c = 105$ MPa, $G_c = 42$ MPa, and shear strength $\tau_c = 1.3$ MPa.

Table 2
Summary of the geometries employed in out-of-plane compression tests for the hierarchical CPL cores, along with the predicted and measured failure strength and collapse modes. SB = shear buckling; FW = face sheet wrinkling; and FC = face sheet crushing.

Specimen/pattern	l_1 (mm)	l_2 (mm)	b (mm)	t_f (mm)	t_c (mm)	Relative density (%)	Predicted failure mode	Predicted strength (MPa)	Measured strength/observed failure mode (MPa)
A/I	16.97	11.5	3	0.3	4	1.64	FW FC SB	1.08 1.38 1.46	0.84/FW
B/II	16.97	13	3	0.6	4	2.59	FW FC SB	2.04 2.6 1.36	1.15/SB

3.2. Stiffness of hierarchical CPL cores

The effective nominal stiffness of the hierarchical CPL cores is analyzed through the deformation of a single foam sandwich strut, as shown in Fig. 5. For a displacement δ imposed in the through-thickness direction, considering all bending and shear deformations besides stretching [12], the axial and shear force, F'_a and F'_s, in the sandwich strut are given as:

$$F_a = A_{sand}\frac{\delta \sin\omega}{l_1} \tag{5}$$

$$F_s = \frac{\delta \cos\omega}{\frac{l_1^3}{12D_{sand}} + \frac{l_1}{S_{sand}}} \tag{6}$$

where $A_{sand} = 2E_f^{eq}bt_f$ is the compressive stiffness of the foam core sandwich strut, $S_{sand} = G_c b t_c$ is the shear stiffness, and D_{sand} is the bending stiffness. For Pattern I, $D^I_{sand} = \frac{1}{6}E_f^{eq}t_f b^3$; while for Pattern II, $D^{II}_{sand} = \frac{1}{2}E_f^{eq}bt_f t_c^2$.

The total force F' in the through-thickness direction is given as:

$$F = F_a \sin\omega + F_s \cos\omega = \delta\left[\frac{\sin^2\omega}{\frac{l_1}{A_{sand}}} + \frac{\cos^2\omega}{\frac{l_1^3}{12D_{sand}} + \frac{l_1}{S_{sand}}}\right] \tag{7}$$

The effective nominal compressive stiffness is given by:

$$E = \frac{2(l_1\sin\omega + X_1)}{\left[l_1\cos\omega + l_2 - X_1\tan\frac{\omega}{2}\right]^2}\left(\frac{\sin^2\omega}{\frac{l_1}{A_{sand}}} + \frac{\cos^2\omega}{\frac{l_1^3}{12D_{sand}} + \frac{l_1}{S_{sand}}}\right) \tag{8}$$

Besides the common axial compression and bending of sandwich struts, shear deformation of foam core will also contribute to the compressive stiffness of the hierarchical CPL cores. The corresponding specific stiffness decreases comparing with that of similar built non-hierarchical CPL structures without foam, mostly due to the weight penalty of the foam core.

3.3. Failure modes and strength predictions

Foam sandwiches of length l_1 that form the higher-order pyramidal core are assumed to have a clamped boundary condition. Based on previous strength analysis for higher-order stretch–stretch-hybrid CPL [15], five competing failure modes will be considered for the bend–stretch-hybrid CPL cores here. These failure modes include face sheet crushing (FC) and face wrinkling (FW) of foam sandwich struts, core shear failure (CSF), and Euler buckling (EB) or shear buckling (SB) of sandwich struts. Theoretical predictions for the corresponding collapse loads are presented below.

Face sheet crushing of sandwich struts: Face sheets of thickness t_f (for foam sandwich struts) of the CPL cores may crush when the compressive stress in the face sheets reaches the crush strength σ_f. The collapse strength of the CPL cores is:

$$\sigma = \frac{4\sigma_f bt_f \sin\omega}{\left[l_1\cos\omega + l_2 - X_1\tan\frac{\omega}{2}\right]^2}\left[1 + \frac{\cos^2\omega}{\sin^2\omega A_{sand}\left(\frac{l_1^2}{12D_{sand}} + \frac{1}{S_{sand}}\right)}\right] \tag{9}$$

Face sheet wrinkling of sandwich struts: The maximum load-induced wrinkling of the inclined sandwich strut can be expressed (like the end-compressed straight sandwich column) as $F_a = (E_f E_c G_c)^{1/3} b t_f$ [18]. Hence, the peak strength of the CPL cores is

$$\sigma = \frac{2(E_f E_c G_c)^{1/3} bt_f \sin\omega}{\left[l_1\cos\omega + l_2 - X_1\tan\frac{\omega}{2}\right]^2}\left[1 + \frac{\cos^2\omega}{\sin^2\omega A_{sand}\left(\frac{l_1^2}{12D_{sand}} + \frac{1}{S_{sand}}\right)}\right] \tag{10}$$

Shear failure of foam core: In out-of-plane compression, shear forces in the sandwich strut can trigger shear failure of foam cores, and the shear force in the foam sandwich strut is given by $F'_s = \tau_c t_c b$. Thus, the peak strength of the stretch–bend-hybrid CPL cores in out-of-plane compression is:

$$\sigma = \frac{2\tau_c t_c b\cos\omega}{\left[l_1\cos\omega + l_2 - X_1\tan\frac{\omega}{2}\right]^2}\left[1 + \frac{\sin^2\omega A_{sand}\left(\frac{l_1^2}{12D_{sand}} + \frac{1}{S_{sand}}\right)}{\cos^2\omega}\right] \tag{11}$$

where τ_c is the foam shear strength.

Euler buckling of sandwich struts: Euler buckling involves bending of the sandwich strut and is a possible failure mode as the CPL core is compressed. The Euler buckling load for built-in Euler columns is $F_a = 4\pi^2 D_{sand}/l_1^2$. The peak compressive strength of the CPL core is given by:

$$\sigma = \frac{8\pi^2 D_{sand}\sin\omega}{l_1^2\left[l_1\cos\omega + l_2 - X_1\tan\frac{\omega}{2}\right]^2}\left[1 + \frac{\cos^2\omega}{\sin^2\omega A_{sand}\left(\frac{l_1^2}{12D_{sand}} + \frac{1}{S_{sand}}\right)}\right] \tag{12}$$

Shear buckling of sandwich struts: Shear buckling of the sandwich struts is determined by the foam shear stiffness, and occurs at a load $F_a = G_c t_c b$. Thus, the compressive failure strength in this mode is

$$\sigma = \frac{2G_c t_c b\sin\omega}{\left[l_1\cos\omega + l_2 - X_1\tan\frac{\omega}{2}\right]^2}\left[1 + \frac{\cos^2\omega}{\sin^2\omega A_{sand}\left(\frac{l_1^2}{12D_{sand}} + \frac{1}{S_{sand}}\right)}\right] \tag{13}$$

3.4. Collapse mechanism maps

Collapse mechanism maps are useful to understand and predict the dominant failure modes and to illustrate the corresponding domains. Maps were constructed as a function of foam relative

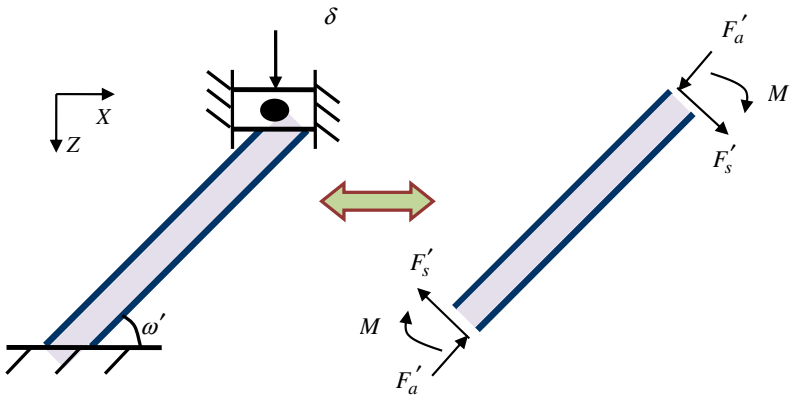

Fig. 5. The loading conditions of a single hollow CPL sandwich strut in *Z*-direction.

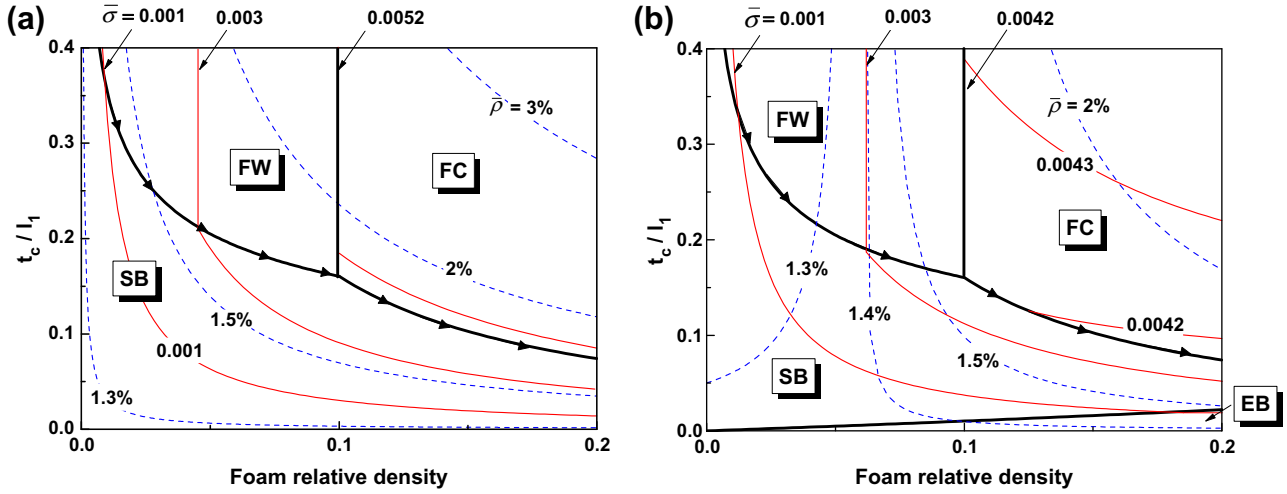

Fig. 6. Failure mechanism maps of the (a) Pattern-I and (b) Pattern-II hierarchical CPL cores with foam sandwich struts in out-of-plane compression ($b/l_1 = 0.177$, $t_f/l_1 = 0.0177$).

density $\bar{\rho}_c$ (0–0.2) and t_c/l_1 (0–0.4) for Patterns I and II with the same $b/l_1 = 0.177$, $t_f/l_1 = 0.0177$ (face sheet thickness $t_f = 0.3$ mm and strut length $l_1 = 16.97$ mm) and incline angle $\omega = 45°$. As shown in Fig. 6, core shear failure (CSF) does not appear in the collapse mechanism maps for either Pattern I or II cores. Three failure modes: FC, FW, and SB, dominate the collapse mechanism map of Pattern-I CPL cores. In contrast, four failure modes together with EB are possible for Pattern-II CPL cores, although EB is possible only for $t_c/l_1 < 0.03$. However, if we assume that the foam generally employed in sandwich structures is thicker than 2 mm ($t_c/l_1 > 0.12$ in the map), the practical failure modes in collapse mechanism maps for Patterns I and II are identical. The boundaries between SB, FC and FW are the same for Patterns I and II.

4. Structural efficiency of hierarchical CPL cores

4.1. Strength of an optimized hierarchical CPL cores

It is instructive to compare the structural efficiency of the stretch–bend-hybrid hierarchical CPLs with stretch–stretch-hybrid counterparts and other lower-order competing constructions, using the structural peak strength at a given relative density as a metric. The optimization problem is based on the collapse mechanism maps, since optimal designs should lie along the boundaries of the collapse regimes where two failure modes are equally likely. Contours of normalized strength $\bar{\sigma} \equiv \sigma/\sigma_f$ (red[1] curves) and relative density $\bar{\rho} \equiv \rho^*/\rho_f$ (blue curves) are added to the maps to convey structural properties associated with the failure mode transitions. These contours can indicate the pathways of optimal designs (arrows in Fig. 6) that maximize the compressive strength for any given relative density. However, EB cannot be an optimized failure mode for Pattern-II CPL cores because the strength does not vary along the EB-FC boundary even as the relative density increases. Increasing buckling resistance is the primary motivation behind hierarchical construction, and thus EB should not occur for an optimized CPL structure in the present study.

To achieve an optimal design, we select the foam core density and sandwich strut geometry that minimizes the relative density of CPL cores for a given strength. Varying the length of the horizontal truss l_2 in the pyramidal core will introduce different knockdown coefficients for compressive strength [15]. We eliminate these effects by setting $l_2 = 0$. The optimal foam core density is obtained via Eqs. (9) and (10) by:

$$\bar{\rho}_c = \left(-0.4 + (0.16 + 1.44(64\sigma_f^3 E_f^{-1} E_s^{-2}/3)\text{^}0.5)\text{^}0.5\right)/0.72 \qquad (14)$$

[1] For interpretation of color in Figs. 1–8, the reader is referred to the web version of this article.

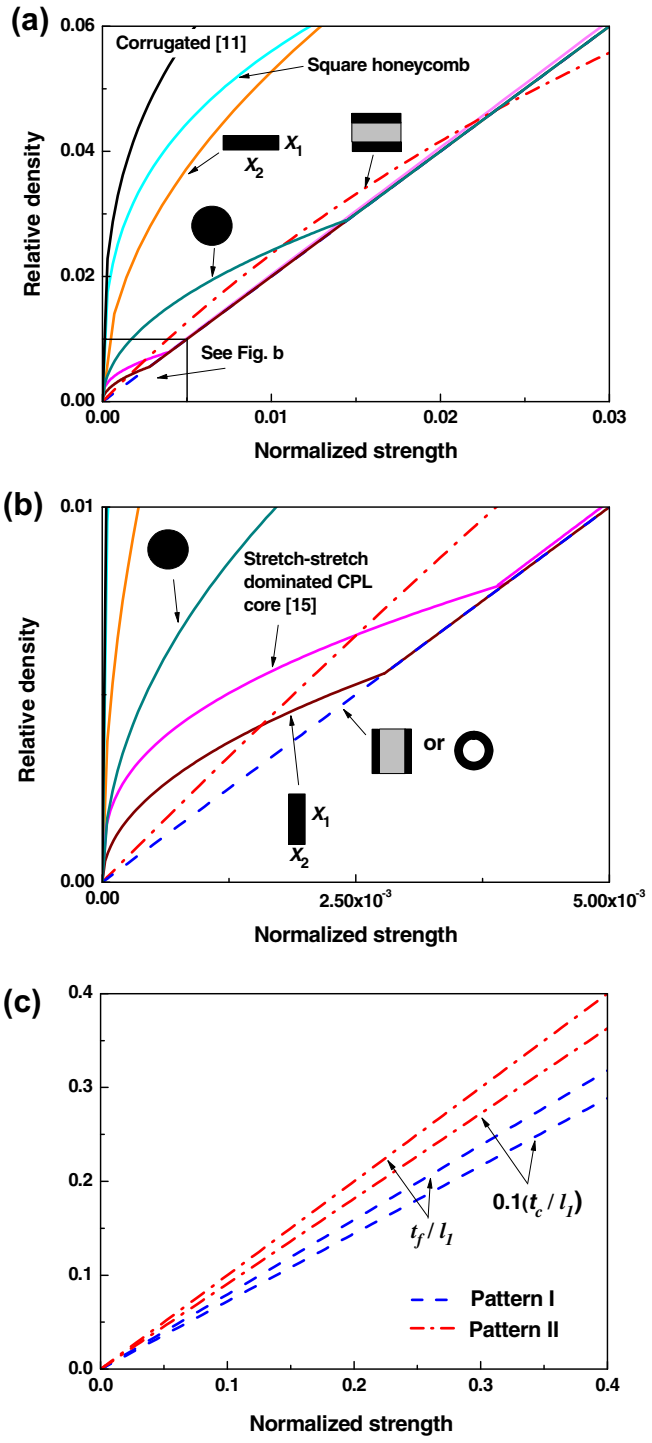

Fig. 7. (a) Variation of relative density with normalized strength for hierarchical CPL cores with foam sandwich struts compared with other competing sandwich cores; (b) Enlarged figure in (a); and (c) Optimal values of t_f/l_1 and t_c/l_1 versus normalized strength. Note that the sketches inside (a) and (b) represent different strut cross-section of pyramidal lattice cores.

The relationship between relative density and normalized peak strength for fully optimized hierarchical CPL cores is plotted in Fig. 7a for Patterns I and II. Pattern-I CPL cores are more efficient than Pattern-II cores when the relative density is below ~4.5%. This is the domain where Euler buckling generally controls failure, which was the primary motivation for employing hierarchical construction. The optimal geometrical parameters t_f/l_1 and t_c/l_1 are plotted in Fig. 7c. These parameters reaffirm that Pattern-II CPL cores require more material (greater equivalent density) than Pattern I to achieve the same load-carrying capacity.

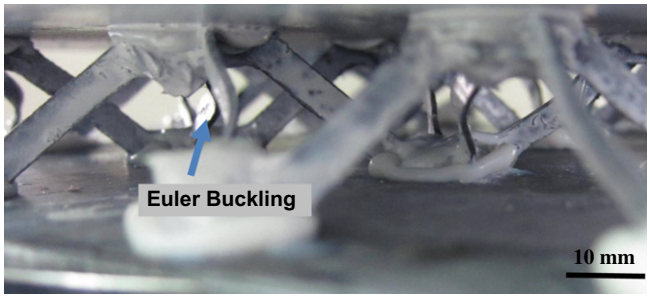

Fig. 8. Failure mode of solid CPL cores with $X_1/X_2 = 5$ in out-of-plane compression.

4.2. Comparison with competing constructions

The featured stretch–bend-hybrid CPL cores with foam sandwich struts described above are non-self-similar hierarchical structures. It is noted that all the comparisons about structural efficiency as following are at low density regime when non-hierarchical structures are easy to buckle. We now first compare their structural efficiency with corresponding solid CPLs of rectangular cross-section (without foam cores), selecting laminate thickness $t = 2t_f = 0.6$ mm. This leads to two stacking patterns similar to those in Fig. 1: in one (in-plane stacking), $X_1/X_2 = 5$, while in the other (out-of-plane stacking), $X_1/X_2 = 1/5$. Note that for comparison, all indices are normalized by face sheet properties of sandwich struts in the present study. The solid CPLs of $X_1/X_2 = 5$ are far more efficient than those of $X_1/X_2 = 1/5$ in out-of-plane compression (see Fig. 7a), which is attributed to the higher bending stiffness $D = E_f X_2 X_1^3/12$ of the former construction ($X_1/X_2 = 5$). This construction can be almost as efficient as Pattern-I hierarchical CPLs when the relative density is >0.5%, but is otherwise less efficient, as shown in Fig. 7b. However, both Patterns I and II hierarchical structures can be more efficient than solid CPLs ($X_1/X_2 = 1/5$).

Because solid CPLs in which $X_1/X_2 = 5$ exhibit high efficiency, we carried out out-of-plane compression tests on these structures. Test results showed that structures with the same strut thickness as that in [6] buckled as well (as shown in Fig. 8), and the peak strength did not increase as expected. We attributed this finding to the difficulty in making the struts stand vertically on the face sheets while assembling the pyramidal core. The struts were too thin (0.6 mm) and did not fit snugly in the cross-slots (width = 1 mm, machine limit). Thus, upon loading in the through-thickness direction, there was also a load component normal to the plane of each strut. No problem will exist for the hierarchical CPL core with thicker foam sandwich struts.

The hierarchical CPL cores were far more efficient than traditional square honeycomb and corrugated cores [11]. The Pattern-II hierarchical CPL core was as efficient as the optimized hollow CPLs, and the Pattern-I hierarchical CPL core was more efficient than solid CPL except when the relative density is $2.5\% < \bar{\rho} < 4.5\%$. The behavior of the same-order stretch–stretch-hybrid hierarchical CPL cores [15] were also included in Fig. 7 to compare with hierarchical CPL cores here. The optimized Pattern-I hierarchical CPL cores with foam sandwich struts were as efficient as the stretch–stretch-hybrid CPL cores. Similarly, the optimized Pattern-II hierarchical CPL cores were less efficient than the stretch–stretch-hybrid CPL cores when the relative density was $0.65\% < \bar{\rho} < 4.5\%$. Note that in the present study the stretch–stretch-hybrid CPL was not superior to the lower-order optimized hollow CPLs, because the efficiency of former structures depended

on the mechanical properties of carbon fiber composites which were different from those reported previously [15].

5. Conclusions

Novel stretch–bend-hybrid hierarchical CPL cores were produced using low-cost foam-core materials. The strut length scale of the hierarchical CPL core was equal to that of traditional CPL cores of lower order [4–9]. Sandwich specimens for two configurations with selected geometries were fabricated and tested in out-of-plane compression. Analytical models for five competing failure modes were used to predict the peak collapse strength and to construct collapse mechanism maps. The predicted values were similar to the measured values for prototype specimens. Foam core shear failure (CSF) did not occupy any domain in the collapse mechanism maps, indicating that the lower-order core construction, stretch- or bend-dominated, had a negligible effect on the macroscopic structural behavior.

Structural efficiencies of the two optimized configurations were compared with almost all pyramidal lattices at present and other traditional core constructions. In-plane stacked hierarchical CPL cores (Pattern-I) were more efficient than out-of-plane stacked cores (Pattern-II) in the domain of greatest interest for hierarchical construction. Similar results were obtained for corresponding solid CPLs without foam. Pattern-I hierarchical CPLs were nearly as efficient as similarly stacked solid CPLs ($X_1/X_2 = 5$), although the measured properties of the latter materials were limited by fabrication methods. The hierarchical structures developed in the present study also performed as efficiently as optimized stretch–stretch hierarchical CPLs of the same order and hollow CPLs of lower-order. All pyramidal lattice or their hierarchical structures in the present study outperformed traditional square honeycomb and corrugated sandwich cores.

The use of low-cost foam in the present study reduced the length scale of the hierarchical cores below that of previous hierarchical constructions [11,15]. As a result, the hierarchical structures here will be more practical for conventional length scale sandwich structural application. Such pyramidal lattice cores can be among the most efficient sandwich cores. The construction concept also provides a pathway to design lattice materials with multifunctional characteristics by the use of specialty foams or judicious selection of equivalent substitutes. The techniques used to fabricate the CPL cores were both simple and relatively accessible, factors that indicate the potential for design and production of high-efficiency and multifunctional cores.

Acknowledgements

The present work is supported by NSFC (90816024 and 10872059), 973 Program (No. 2011CB610303), Program of Excellent Team in HIT. S.N. gratefully acknowledges support from the Gill Composites Center. S.Y. also acknowledges the support of Most Potential New Scholar Prize awarded by Ministry of Education in China (AUDQ1010000511) and the support from China Scholarship Council (CSC) during the visit at University of Southern California.

References

[1] Evans AG, Hutchinson JW, Fleck NA, Ashby MF, Wadley HNG. The topological design of multifunctional cellular metals. Prog Mater Sci 2001;46(3–4):309–27.
[2] Yin S, Ma L, Wu LZ. Carbon fiber composite lattice structure filled with silicon rubber. Procedia Eng 2011;10:3191–4.
[3] Fan HL, Meng FH, Yang W. Mechanical behaviors and bending effects of carbon fiber reinforced lattice materials. Arch Appl Mech 2006;75(10–12):635–47.
[4] Yin S, Wu L, Ma L, Nutt S. Hybrid truss concepts for carbon fiber composite pyramidal lattice structures. Compos B – Eng 2012;43(4):1749–55.
[5] Wang B, Wu LZ, Ma L, Sun YG, Du SY. Mechanical behavior of the sandwich structures with carbon fiber-reinforced pyramidal lattice truss core. Mater Des 2010;31(5):2659–63.
[6] Xiong J, Ma L, Wu LZ, Wang B, Vaziri A. Fabrication and crushing behavior of low density carbon fiber composite pyramidal truss structures. Compos Struct 2010;92(11):2695–702.
[7] Finnegan K, Kooistra G, Wadley HNG, Deshpande VS. The compressive response of carbon fiber composite pyramidal truss sandwich cores. Int J Mater Res 2007;98(12):1264–72.
[8] Moongkhamklang P, Deshpande VS, Wadley HNG. The compressive and shear response of titanium matrix composite lattice structures. Acta Mater 2010;58(8):2822–35.
[9] Yin S, Wu L, Ma L, Nutt S. Pyramidal lattice sandwich structures with hollow composite trusses. Compos Struct 2011;93(12):3104–11.
[10] Schaedler TA, Jacobsen AJ, Torrents A, Sorensen AE, Lian J, Greer JR, et al. Ultralight metallic microlattices. Science 2011;334(6058):962–5.
[11] Kooistra GW, Deshpande V, Wadley HNG. Hierarchical corrugated core sandwich panel concepts. J Appl Mech – T ASME 2007;74(2):259–68.
[12] Kazemahvazi S, Zenkert D. Corrugated all-composite sandwich structures. Part 1: modeling. Compos Sci Technol 2009;69(7–8):913–9.
[13] Kazemahvazi S, Tanner D, Zenkert D. Corrugated all-composite sandwich structures. Part 2: failure mechanisms and experimental programme. Compos Sci Technol 2009;69(7–8):920–5.
[14] Cote F, Russell BP, Deshpande VS, Fleck NA. The through-thickness compressive strength of a composite sandwich panel with a hierarchical square honeycomb sandwich core. J Appl Mech – T ASME 2009;76(6).
[15] Yin S, Wu LZ, Nutt S. Structural efficiency of hierarchical composite lattice cores, submitted for publication.
[16] ASTM: C365/C 364M-05. Standard test method for flat wise compressive properties of sandwich cores. Weat Conshohocken (PA): ASTM Int.; 2006.
[17] Gibson LJ, Ashby MF. Cellular solids: structure and properties. 2nd ed., Cambridge University Press; 1999.
[18] Fleck NA, Sridhar I. End compression of sandwich columns. Compos A – Appl Sci 2002;33(3):353–9.